Astronomy in Focus, XXIXB, Focus Meeting 22
XXIXth IAU General Assembly, August 2015
Piero Benvenuti, ed.

doi:10.1017/S1743921316006906

Probing the Cosmic Frontier of Galaxies

Pascal A. Oesch

Yale Center for Astronomy and Astrophysics, Physics and Astronomy Departments, New Haven, CT 06520, USA
email: pascal.oesch@yale.edu

Abstract. Understanding when and how the first galaxies formed and what sources reionized the universe are key goals of extragalactic astronomy. Thanks to deep surveys with the powerful WFC3/IR camera on the HST, the observational frontier of galaxy build-up now lies at only ~ 450 Myr after the Big Bang, at redshifts $z \sim 10-12$. In combination with deep data from Spitzer/IRAC we can now probe the evolution of the stellar mass density over 96% of cosmic history. However, detecting and characterizing galaxies at these early epochs is challenging even for HST and the sample sizes at the earliest redshifts are still very small. The Hubble Frontier Fields provide a prime new dataset to improve upon our current, sparse sampling of the UV luminosity function at $z > 8$ from blank fields to answer some of the most pressing open questions. For instance, even the evolution of the cosmic star-formation rate density at $z > 8$ is still debated. While our measurements based on blank field data indicate that galaxies with SFR>0.7 Msol/yr disappear quickly from the cosmic record between $z \sim 8$ and $z \sim 10$, other previous results, e.g., from the CLASH survey favor a more moderate decline. Here, we briefly review the recent progress in studying galaxy build-up out to $z \sim 10$ from the combined blank field and existing Frontier Field datasets and discuss their implications for primordial galaxy formation and cosmic reionization.

Keywords. galaxies: high-redshift – galaxies: evolution – galaxies: abundances

1. Introduction

Understanding when and how the first galaxies formed is one of the most intriguing and challenging open questions of modern observational astronomy, and it is one of the main science drivers for the Directors Discretionary Time Hubble Frontier Field (HFF) program. Recently, great progress has been made to study early galaxies out to $z \sim 7-8$ (e.g. Bouwens *et al.* 2015). However, beyond that our understanding of galaxies is still limited due to the small sample sizes of $z \sim 9-10$ galaxy candidates. Consequently, how the cosmic star-formation rate density evolves from $z \sim 8$ to $z \sim 10$ is still uncertain and debated. On the one hand, the analysis of the full HUDF09/12 and CANDELS GOODS data revealed a rapid decline of the SFRD by $\sim 10\times$ from $z \sim 8$ to $z \sim 10$ in only 170 Myr (see e.g. Oesch *et al.* 2012, 2014, but see also Ellis *et al.* 2013). However, the two detections of $z > 9$ galaxies in the small volume probed by the CLASH survey (Zheng *et al.* 2012; Coe *et al.* 2013) are consistent with a continued decline according to lower redshift trends (see also McLeod *et al.* 2015).

The HFF program is ideally suited to address this question. It exploits the lensing magnification of six massive foreground clusters in order probe intrinsically very faint sources, fainter than accessible with the deepest *HST* data over the HUDF, but over a small volume. Additionally, the HFF observes six deep parallel blank field pointings, which help to mitigate the uncertainties of magnification maps and cosmic variance.

First results on $z \sim 7-9$ galaxies were already derived with partial HFF data (see e.g. Atek *et al.* 2014; Laporte *et al.* 2014; Zheng *et al.* 2014; Coe *et al.* 2015), and here we present first results on the $z \sim 10$ galaxy population based on the first four HFF clusters.

2. Selection of $z \sim 10$ Galaxies in the HFF Data

In this analysis, we make use of the fully calibrated and reduced v1 HFF dataset of the first four completed clusters and their parallel fields provided by STScI †. This includes deep ACS optical imaging in addition to near-IR WFC3/IR data drizzled to the same pixels at 60 mas scale. The filter set of the HFF program allows for an efficient and reliable selection of galaxies at $z > 9.5$ based on the Lyman Break selection. At these redshifts the Lyα break shifts into the center of the J_{125} filter, resulting in very red $J_{125} - H_{160}$ colors and non-detection in shorter wavelength filters.

Our selection is based on $J_{125} - H_{160} > 1.2$, in addition to non-detections in the optical and Y bands at $< 2\sigma$. Additionally, we ensure that galaxies are not detected in the Spitzer/IRAC imaging, which allows us to remove contamination by evolved or dusty intermediate redshift galaxies. For more information on the selection see, e.g., Oesch *et al.* (2014) and Oesch *et al.* 2015, in prep.

Going through all the four cluster and parallel images of the current HFF release, we identify a total of seven $z > 9.5$ galaxy candidates (Oesch *et al.* 2015, in prep). With the exception of the multiply imaged source behind the cluster A2744 (see also Zitrin *et al.* 2014), all these sources are quite faint, $5-6\sigma$ detections, i.e., close to the detection limit of the data. None of these is seen in the deep Spitzer/IRAC imaging, which makes them bona-fide $z \sim 10$ galaxy candidates. After quantifying the selection volume of all clusters in the next section, we will use these candidates to derive a new, independent estimate of the cosmic SFRD.

3. Expected Galaxy Counts in Lensed Fields

Even at the highest redshifts, galaxies are not point-sources at HST's resolution and they have a finite size (e.g. Oesch *et al.* 2010; Ono *et al.* 2013; Holwerda *et al.* 2015). The limited surface brightness sensitivity of HST therefore leads to a reduction of the selection volume of highly magnified and sheared sources (see e.g. Wong *et al.* 2012; Oesch *et al.* 2015).

We perform extensive source recovery simulations to test this effect and to quantify the source selection volume as a function of position and magnification behind the lensing clusters. This is required in order to use the HFF cluster fields for an estimate of the cosmic star-formation rate density. We follow standard procedures for blank fields and insert artificial galaxies with different light profiles, sizes, luminosities, and redshifts into the original science images. However, for the cluster fields, we apply the position dependent shear to the artificial galaxies before inserting these into the images. After re-running our detection algorithm with the same parameters as for the original images, we can estimate the magnification dependent selection efficiency, $p(z, m, \mu)$. This is given by the fraction of inserted galaxies at magnification μ with redshift z and observed magnitude m, which are both detected and satisfy our color selection criteria. This therefore accounts both for completeness at a given observed magnitude, as well as for photometric scatter which statistically removes galaxies from our LBG color selection box.

Using this selection function, we can compute the number of expected galaxy images (double-counting multiple images) in bins of magnitude for a given UV LF ϕ. An example of this is shown in Figure 1 for the Abell 2744 cluster and parallel fields. Taking into account the reduced completeness due to lensing shear results in a reduction of the total number of $z \sim 10$ galaxies in these clusters by a factor $\sim 1.5-2\times$, and somewhat reduces the power of these clusters to probe to > 30 mag.

† see `http://archive.stsci.edu/pub/hlsp/frontier/`

https://doi.org/10.1017/S1743921316006906 Published online by Cambridge University Press

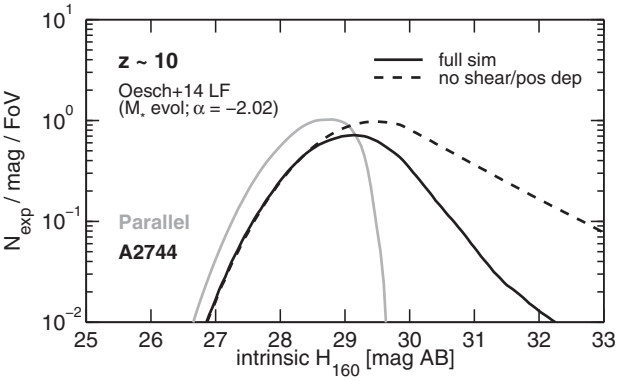

Figure 1. The differential expected number of $z \sim 10$ galaxies to be detected in the HFF data around the cluster Abell 2744 as a function of intrinsic, de-magnified H-band magnitude. The light gray line shows the expectation for the parallel blank field, while the black curves correspond to the field behind the lensing cluster. Thanks to the magnification the cluster field probes to fainter intrinsic magnitudes. However, when accounting for lensing shear in these calculations (solid line with vs. dashed line without), the power of the lensing cluster to push to below > 30 mag is somewhat limited due to reduced completeness in the highest magnification regions (see also Oesch *et al.* 2015). It will be important to include this effect when planning future surveys, e.g., with the JWST.

An additional, very important uncertainty in these calculations is the intrinsic size distribution of highly magnified galaxies, fainter than the detection limits in the parallel fields. The size-luminosity or size-mass relations of star-forming galaxies is surprisingly constant at all redshifts $z = 0 - 3$ seen in the CANDELS dataset ($r_e \propto M^{0.22}$; see van der Wel *et al.* 2014) and we currently have no convincing evidence for a change in these scaling relations at higher redshifts (see e.g. Mosleh *et al.* 2012; Huang *et al.* 2013). Changing the exponent of the size-luminosity relation from $r_e \propto L^{0.22}$ to $r_e = \text{const}$ results in a factor $\sim 2\times$ systematic change in the selection volume at high magnification (see Oesch *et al.* 2015). Thus, it will be extremely important to derive new constraints on the size scaling in the future, potentially making use of the HFF dataset itself (see e.g. Kawamata *et al.* 2015).

4. Results: The Cosmic SFRD at $z \sim 10$

We now combine the first four HFF cluster and blank field images to derive an updated estimate of the cosmic SFRD at $z \sim 10$, by assuming a UV LF shape and varying its normalization to fit the observed number counts in the eight images. This new estimate provides an independent confirmation of our previous measurement based on the HUDF and GOODS fields (Oesch *et al.* 2014).

In Figure 2, we compare the new estimate from the first 4 HFF fields to an average of all previous measurements, and to a whole suite of theoretical models. Clearly, both the empirical evidence and the theoretical models favor a strong evolution in the SFRD indicating that the galaxy population builds up very rapidly in the first 700 Myr (see also Oesch *et al.* 2014).

Note, however, that the rapid decline in the observed SFRD is likely simply a consequence of the fixed detection limit in luminosity. In particular if the faint-end slope of the UV LF evolves further to steeper values as seen at lower redshifts, the *total* SFRD would evolve much more gradually. Such higher total values are likely required to reionize the universe early enough to be consistent with the electron scattering optical depth mea-

https://doi.org/10.1017/S1743921316006906 Published online by Cambridge University Press

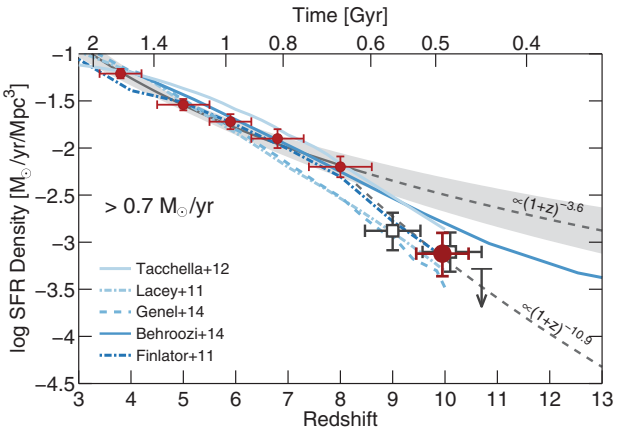

Figure 2. The evolution of the cosmic SFR density to $z \sim 10$. Averages of all previous estimates in the literature at $z > 8$ are shown by the open squares, while the new determination from the first 4 cluster and parallel Frontier Fields is shown as the large filled circle. The 4 HFFs provide a completely independent confirmation of a very rapid drop in the SFRD between $z \sim 8$ to $z \sim 10$ as has previously been claimed from the analysis of blank field data in the GOODS/CANDELS and HUDF fields (see also Oesch *et al.* 2015, in prep). This trend is completely consistent with a whole suite of theoretical predictions (gray labeled curves) when integrating those down to the same detection limit as current observations.

surements in CMB experiments. However, the recent lower values measured by Planck eased some of this tension. Future observations with the JWST will greatly improve on the current SFRD estimates at $z < 11$ and push such observations to beyond $z \sim 12-15$.

References

Atek, H., *et al.* 2014, *ApJ*, 786, 60
Bouwens, R. J., *et al.* 2015, *ApJ*, 803, 34
Coe, D., Bradley, L., & Zitrin, A. 2015, *ApJ*, 800, 84
Coe, D., *et al.* 2013, *ApJ*, 762, 32
Ellis, R. S., *et al.* 2013, *ApJL*, 763, L7
Holwerda, B. W., Bouwens, R., Oesch, P., Smit, R., Illingworth, G., & Labbe, I. 2015, *ApJ*, 808, 6
Huang, K.-H., Ferguson, H. C., Ravindranath, S., & Su, J. 2013, *ApJ*, 765, 68
Kawamata, R., Ishigaki, M., Shimasaku, K., Oguri, M., & Ouchi, M. 2015, *ApJ*, 804, 103
Laporte, N., *et al.* 2014, *AaapA*, 562, L8
McLeod, D. J., McLure, R. J., Dunlop, J. S., Robertson, B. E., Ellis, R. S., & Targett, T. A. 2015, *MNRAS*, 450, 3032
Mosleh, M., *et al.* 2012, *ApJL*, 756, L12
Oesch, P. A., Bouwens, R. J., Illingworth, G. D., Franx, M., Ammons, S. M., van Dokkum, P. G., Trenti, M., & Labbé, I. 2015, *ApJ*, 808, 104
Oesch, P. A., *et al.* 2010, *ApJL*, 709, L21
—. 2012, *ApJ*, 745, 110
—. 2014, *ApJ*, 786, 108
Ono, Y., *et al.* 2013, *ApJ*, 777, 155
van der Wel, A., *et al.* 2014, *ApJ*, 788, 28
Wong, K. C., Ammons, S. M., Keeton, C. R., & Zabludoff, A. I. 2012, *ApJ*, 752, 104
Zheng, W., *et al.* 2012, *Nature*, 489, 406
—. 2014, *ApJ*, 795, 93
Zitrin, A., *et al.* 2014, *ApJL*, 793, L12

https://doi.org/10.1017/S1743921316006906 Published online by Cambridge University Press